IEEE Access
Multidisciplinary | Rapid Review | Open Access Journal

SPECIAL SECTION ON KEY ENABLING TECHNOLOGIES FOR PROSUMER ENERGY MANAGEMENT

Received December 28, 2020, accepted January 11, 2021, date of publication January 18, 2021, date of current version February 1, 2021.

Digital Object Identifier 10.1109/ACCESS.2021.3052349

Novel Fault Location for High Permeability Active Distribution Networks Based on Improved VMD and S-transform

YANCHUN XU[1], CAICAI ZHAO[1], SHASHA XIE[1], AND MI LU[2], (Senior Member, IEEE)
[1]Hubei Provincial Key Laboratory for Operation and Control of Cascaded Hydropower Station, China Three Gorges University, Yichang 443002, China
[2]Department of Electrical and Computer Engineering, Texas A&M University, College Station, TX 77840, USA

Corresponding author: Caicai Zhao (zcc9597@163.com)

This work was supported in part by the National Natural Science Foundation of China under Grant 51707102; and in part by the Key Project of Science and Technology Research Plan of Education Department of Hubei under Grant D20201203.

ABSTRACT Aiming at the problem of the inaccurate fault location in high-permeability active distribution network, a novel method of fault location for active distribution network based on improved variational mode decomposition (IVMD) and S-transform is proposed in this paper. Firstly, the judgment method of instantaneous frequency is adopted to determine the value of decomposition layers k. Meanwhile the algorithm of variational mode decomposition (VMD) is utilized to decompose the fault signal of traveling wave. Then, the kurtosis criterion is employed to select the appropriate intrisic mode functions (IMFS) for S-transform in order to obtain the S-matrix with higher resolution. The high-frequency components in the matrix are extracted to determine the arrival time for the head of the fault traveling wave. Finally, the fault distance can be calculated by the special distance formula without considering the velocity of the traveling wave. The simulations show that the proposed method can accurately measure the fault distance for the transmission lines in high permeability active distribution network, and the measurement error is limited within 200m, which verifies the accuracy and effectiveness of the proposed algorithm.

INDEX TERMS Active distribution network, fault location, fault traveling wave, improved variational mode decomposition (IVMD), S-transform.

I. INTRODUCTION

With the increasing penetration of renewable energy in power system, its uncertainty has a great impact on fault location in distribution networks [1], [2]. The direction of power flow and the operation mode of the grid will be affected after the distributed generation (DG) access to the distribution network. The operating characteristics of DG will be affected by the external environment, which increase the difficulty of fault location in active distribution network. Therefore, it is of great importance to study the problem of fault location in active distribution network with high permeability [3]–[5].

Different from the fault location method of the transmission grids [6], [7], there are still some problems of fault location in active distribution networks. Generally speaking, the methods of fault location can be divided into three categories: the impedance-based methods [8]–[10], the traveling wave-based methods [11]–[15] and the machine learning-based methods [16]. In [8], an improved impedance method is proposed to solve the problem of equivalent impedance impact due to DG access, in which the fault location equation is established based on the feature of zero reactive power for the transition impedance. However, it is necessary to iterate continuously during the process of the solution to ensure more accurate results, and the process of the calculation is more complicated. The equations of the fault loop and the models of optimal estimation are established and the speed of the algorithms are faster [9]. Meanwhile, DG access is more independent, but it is vulnerable to the currents of the residual voltage in the loads. The traveling wave-based methods are mainly to measure the time of the wave head for the traveling wave accurately. The arrival time difference of traveling wave is adopted to locate the fault point and the path matrix of traveling wave is established. But the large number of synchronization measurement devices in the system increases the operating cost and it is not applicable to active distribution network with DG access [12]. Based on [12], a search matrix of fault branch is built and the influence of DG access on the head of the initial traveling wave in the fault is considered [13]. The time difference between the

The associate editor coordinating the review of this manuscript and approving it for publication was Huai-Zhi Wang.

This work is licensed under a Creative Commons Attribution 4.0 License. For more information, see https://creativecommons.org/licenses/by/4.0/

wave head arrival of the line mode and the wave head arrival of the zero mode is utilized to calculate the fault distance in the active distribution network. However, the zero mode attenuation is more serious during the transmission process, which will lead to inaccurate measurement results [14]. The machine learning-based methods including using neural network to achieve fault location [16]. Fault location can be realized through simulation calculation of big data and neural network. However, when the structure of the distribution network changes, especially after DG is connected, the mathematical model is no longer applicable, resulting in inaccurate positioning. In [17], three fault location methods are proposed based on electromagnetic time reversal (EMTR) under the AC lines, but the errors calculated by the methods are large, and the algorithm is not applicable for active distribution network, because the access of DG will affect the establishment of the fluctuation equation in the electromagnetic transient process.

Empirical mode decomposition (EMD) is an adaptive iterative filtering algorithm, it can deal with the fault signals, but will cause the phenomenon of the end effect and mode aliasing [18]. Based on EMD, the ensemble empirical mode decomposition (EEMD) is brought out [19], which can only inhibit the phenomenon of mode alising, but cannot completely eliminate it. Compared with EMD and EEMD, variational mode decomposition (VMD) is an algorithm for non-stationary signal decomposition [20]. Its essence is a set of wiener filters that can eliminate the modal mixing during the iterative filtering process [21]. S-transform is a local time and frequency method, which has the advantages of wavelet transform and Fourier transform. Since the traveling wave signal is a non-stationary high-frequency transient signal, susceptible to interference from noise, and there are difficulties in detecting the signal. Therefore, the accurate detection of the traveling wave head and its corresponding moment are the key to traveling wave methods. S-transform is the effective method to extract the features of non-stationary signals. It gives the higher resolution matrix, which can accurately identify the arrival time of the traveling wave head. Higher accuracy can be achieved even under larger disturbance and noise after DG access to the distribution network [22]–[24].

In summary, this study combines VMD and S-transform and optimizes the corresponding parameters to propose a fault location method for high permeability active distribution network based on IVMD and S-transform. The method is mainly aimed at the feature that the fault signal in active distribution network is a non-stationary signal. The number of VMD decomposition layers k is optimized by the instantaneous frequency method, and the signal is decomposed into k intrisic mode functions (IMFS). The kurtosis criterion [25], is used to select the appropriate IMF to perform S-transform, after which the matrix with high-frequency components can be extracted to determine the arrival time of fault traveling wave head, and finally the fault distance is calculated by substituting into the distance calculation formula. Through extensive simulations, the proposed method can accurately measure the fault distance in the multi-branch high permeability active distribution network model.

II. VARIATIONAL MODE DECOMPOSITION

A. BASIC PRINCIPLES OF VMD

Due to the randomness and intermittence of DG [26], the uncertainty of DG access to distribution network will affect the extraction of fault signal in active distribution network, which is non-stationary. The algorithm VMD is used for the process of decomposing the non-stationary into k intrinsic mode functions (IMFS) with abundant fault signals, which can solve the problems of disturbance and uncertainty caused with DG access. The construction of the variational problems is as follows.

Based on the squared-norm of the demodulated signal in the baseband, the spectral bandwidth of each IMF is estimated from the component of positive frequency which is obtained from the Hirbert transform. The specific constraint model is shown as follows:

$$\min_{\{\mu_k\},\{\omega_k\}} \left\{ \sum_k \left\| \partial_t \left[\left(\delta_t + \frac{\mathrm{j}}{\pi t} \right) \mu_k(t) \right] e^{-\mathrm{j}\omega_k t} \right\|_2^2 \right\} \tag{1}$$

where:

$\{\mu_k\} = \{\mu_1, \mu_2, \cdots, \mu_k\}$ is the kth mode component of the decomposition;
$\{\omega_k\} = \{\omega_1, \omega_2, \cdots, \omega_k\}$ is the center frequency of all IMF components;
∂_t is the partial derivative of t;
δ_t is the impulse function.

The Lagrange multiplier operator is introduced to solve the optimal solution of (1), as shown in (2):

$$\begin{aligned} &L(\{\mu_k\}, \{\omega_k\}, \lambda) \\ &= \alpha \sum_k \left\| \partial_t \left[\left(\delta(t) + \frac{\mathrm{j}}{\pi t} \right) \mu_k(t) \right] e^{-j\omega_k t} \right\|_2^2 \\ &\quad + \left\| f(t) - \sum_k \mu_k(t) \right\|_2^2 + \langle \lambda(t), f(t) - \sum_k \mu_k(t) \rangle \end{aligned} \tag{2}$$

where:

λ is the Lagrange multiplier operator;
α is the penalty factor;
$f(t)$ is the signal to be decomposed.

The alternative direction method of multipliers (ADMM) is adopted to solve the above variational problem, and the "saddle point" in (2) is obtained by updating the iterations μ_k^{n+1}, ω_k^{n+1}, and λ^{n+1}. The symbol $\wedge$ is the value of the solution converted to the frequency domain by using the Parseval/Plancherel Fourier isometric transform. The optimal solution and the updated central frequency of each μ_k can be expressed as follows:

$$\hat{\mu}_k^{n+1}(\omega) = \frac{\hat{f}(\omega) - \sum_{i \neq k} \hat{\mu}_k(\omega) + \frac{\hat{\lambda}(\omega)}{2}}{1 + 2\alpha(\omega - \omega_k)^2} \tag{3}$$

$$\omega_k^{n+1} = \frac{\int_0^\infty \omega \left| \hat{\mu}_k(\omega) \right|^2 d\omega}{\int_0^\infty \left| \hat{\mu}_k(\omega) \right|^2 d\omega} \tag{4}$$

where:

$\hat{\mu}_k^{n+1}(\omega)$ is the Wiener filter of the k-th component, and $\mu_k(t)$ is the real part of the Wiener filter;
ω_k^{n+1} is the center frequency value of the corresponding component.

The specific steps of VMD decomposition are as follows:

1) The initial value is set: Firstly set the initial value of $\{\hat{\mu}_k^1\}$, $\{\hat{\omega}_k^1\}$, $\hat{\lambda}^1$and n to 0, and $n = n+1$. Meanwhile, k is the number of VMD decomposition layers;
2) The parameters are updated: the formula (3) and (4) are used to update the value$\mu_k$andω_k. The value$\hat{\lambda}$is updated by (5):

$$\hat{\lambda}^{n+1}(\omega) \leftarrow \hat{\lambda}^n(\omega) + \tau\left(\hat{f}(\omega) - \sum_{k=1}^{K}\hat{\mu}_k^{n+1}(\omega)\right) \tag{5}$$

where, τ is the update parameter, which can be set to 0 while the fidelity of decomposition results is not high.
3) The parameter is iterated to convergence: While the set discriminative accuracy $\varepsilon > 0$ satisfies the formula (6), the iterative process will end. The k modal components $\mu_k(t)$can be obtained by the inverse Fourier transform of $\mu_k(\omega)$, and the results are output. Otherwise, it returns to the steps 1) and 2) and continues the iteration until (6) is satisfied.

$$\sum_k \left\|\hat{\mu}_k^{n+1} - \hat{\mu}_k^n\right\|_2^2 \Big/ \left\|\hat{\mu}_k^{n+1}\right\|_2^2 < \varepsilon \tag{6}$$

B. IMPROVED VARIATIONAL MODE DECOMPOSITION

The determination for the number of decomposition layers k is crucial as VMD decomposition of the signals is performed. If the value k is chosen inappropriately, the decomposition results will be affected. It will lead to incomplete decomposition if the value k is too small. Similarly, over-decomposition will occur if the value k is too large. Therefore, the key point of VMD decomposition is to choose the appropriate number of decomposition layers.

The method of instantaneous frequency judgment is employed in this study to select the value k [27]. Assuming that there are M sampling points in the i-th modal component of the signal to be decomposed and the instantaneous frequency of the j-th sampling point is calculated to obtain the frequency f_{ij}. The value k is set and Hilbert transform is performed on the modal components after VMD decomposition in order to obtain the analytical signal of each IMF component. Moreover, the instantaneous frequency of each IMF component is calculated by using the function *instfreq*, and the solution is solved by (7):

$$f_i = \frac{1}{N}\sum_j f_{ij} \tag{7}$$

In this study, the VMD decomposition is carried out based on the location model of the multi-terminal traveling wave.

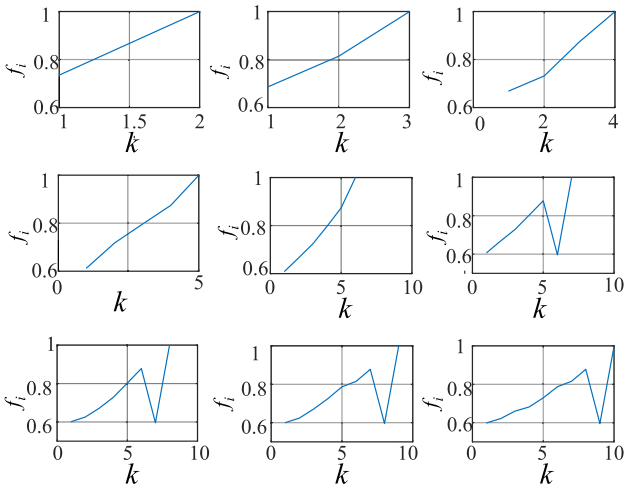

FIGURE 1. Instantaneous frequency mean under the different k values.

Firstly, the value k is set from 1 to 9, and then the instantaneous frequency is found out by using the method of instantaneous frequency judgment. Nine curves of instantaneous frequency mean can be obtained, as shown in Fig. 1.

It shows in Fig.1 that the trend of the curve changes as the value k reaches a certain value and the critical value corresponding to the time of shift occurrence is the optimal value k. It can be seen from the sixth subplot that the instantaneous frequency drops sharply while the value k equals 6. Therefore, the best decomposition level is $k = 5$. If the value k is too large, the instantaneous frequency of IMF changes greatly and over-decomposition occurs; otherwise, the instantaneous frequency changes little and incomplete decomposition appears. Thus, the method of instantaneous frequency judgment is utilized to select a more suitable value k so that the parameters of VMD can be optimized.

III. EXTRACTION METHOD OF FAULT TRAVELING WAVE

A. KURTOSIS CRITERION

The parameter kurtosis is used to describe the sharpness of the waveform, which is dimensionless and reflects the vibration of the signal during the fault. The mathematical expression is given as follows:

$$\mathrm{Ku} = \frac{E(x-\mu)^4}{\sigma^4} \tag{8}$$

where:

x is the fault signal;
σ is the standard deviation of the signal x;
μ is the mean value of the signal x;
E is the mathematical expectation.

It can be seen from (8) that Ku represents the fourth-order mean value of the signal.

The value Ku of kurtosis is about three while the fault signal obeys the normal distribution and the value Ku is about zero while the signal obeys the average distribution, the value of kurtosis for the fault signal will be greater than three while the fault occurs in distribution network [25]. The larger the value of kurtosis is, the more the impulse components in

the fault occurs and the easier the fault characteristics are extracted. The value of kurtosis for each mode component is calculated after VMD decomposition for the fault traveling wave, and the component with the larger value kurtosis is selected for the next decomposition.

B. S-TRANSFORM

S-transform is proposed by R.G.Stockwell [28], and it is the effective method to extract the features of non-stationary signals. It is the development of wavelet transform and short-time Fourier transform, and it has the advantages of better time-frequency characteristics and different frequency resolution. S-transform is adopted for feature extraction of IMFS with the larger values of kurtosis to obtain a high resolution S-matrix which avoids the phenomenon of low time resolution. The matrix reflects some characteristics of fault signals in active distribution network and improving the resolution of S-transform in time, and the arrival time for the head of the fault traveling wave reaches the detection point is more accurate. The elements of the matrix reflect the variation of the signal in amplitude and phase at the different frequencies.

The one-dimensional continuous S-transform of the signal $x(t)$ is given as follows:

$$S(\tau,f)=\int_{-\infty}^{\infty}x(t)\omega(t-\tau,f)\,e^{-\mathrm{i}2\pi ft}\mathrm{d}t \tag{9}$$

where:

$$\omega(t-\tau,f)=\frac{|f|}{\sqrt{2\pi}}e^{\frac{-(t-\tau)^2f^2}{2}};$$

$S(\tau,f)$ is the S-matrix;
$\omega(t-\tau,f)$ is the Gaussian window function;
τ is the translation factor on this window function, which is used to control the position of the Gaussian window on the time axis t;
f is the frequency;
i is the imaginary unit;

The original signal $x(t)$ can be obtained by inverse transformation of a signal in (9) as follows:

$$x(t)=\int_{-\infty}^{\infty}\left[\int_{-\infty}^{\infty}S(\tau,f)\,\mathrm{d}\tau\right]e^{\mathrm{i}2\pi ft}\mathrm{d}f \tag{10}$$

It can be seen that the S-transform overcomes the short-time Fourier Gaussian window and the defect of height fixation. Meanwhile, the discrete form of the S-transform are given as follows:

$$S[m,n]=\sum_{0}^{N-1}X[n+k]\bullet e^{-2\pi^2k^2/n^2}\bullet e^{\mathrm{i}2\pi km/N}\quad(n\neq 0) \tag{11}$$

$$S[m,n]=\frac{1}{N}\sum_{k=0}^{N-1}x[k]\quad(n=0) \tag{12}$$

where:

$$X[n]=\frac{1}{N}\sum_{k=0}^{N-1}x[k]\bullet e^{-\mathrm{i}2\pi kn/N};$$

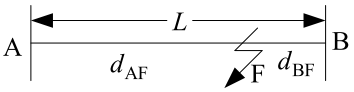

FIGURE 2. Schematic diagram of two-terminal location.

$S[m,n]$ is the corresponding S-matrix. The abscissa represents time and the ordinate represents frequency;
$x[k]$ is the discrete vector of $x(t)$;
N is the total number of sampling points;
n is the sampling frequency point and $n=0,1,\cdots,N-1$.

The actual frequency of each point is $f=\left(f_s/N\right)*n$, and f_s is the sampling frequency.

The matrix of S-transform can be obtained by (11) and (12), which can be expressed as (13):

$$S(m,n)=A(m,n)\,e^{jp(m,n)} \tag{13}$$

where:

$A(m,n)$ is the amplitude matrix;
$p(m,n)$ is the phase angle matrix.

The rows of the S-matrix represent the variation of amplitude or phase angle at a certain frequency with the time, and the columns of the S-matrix represent the variation of amplitude or phase angle at a certain moment with the frequency. According to the characteristics of the S-matrix, the high frequency components are selected to identify the mutation point of the fault and determine the head of the fault traveling wave in active distribution system.

IV. FAULT LOCATION SCHEME

A. TWO-TERMINAL LOCATION METHOD

The basic principle of two-terminal fault location is to determine the fault distance by using the initial time of the head arrival for the fault traveling wave detected at both ends of the line and the traveling wave velocity. The principle of the two-terminal fault location is shown in Fig. 2.

When the fault occurs at the point F, the distance from fault point F to the ends A and B is calculated as (14) by using the principle of two-terminal traveling wave location as follows:

$$\begin{cases}d_{AF}=\dfrac{L+v(t_A-t_B)}{2}\\ d_{BF}=\dfrac{L+v(t_B-t_A)}{2}\end{cases} \tag{14}$$

where:

L is the length of line AB;
v is the wave velocity of the traveling wave while the fault occurs;
t_A and t_B are the time required for the transmission of the initial traveling velocity to both ends of A and B, respectively.

According to (14), the fault distance is related to the velocity of the traveling wave and the transmission time at the wave head at the time of the fault. In the actual distribution network, the change of temperature and climate will affect

the length of the line, and the parameters of the line will change because some information from the line in the distribution network is not accurate. Thus there will be a certain impact on the velocity of the traveling wave, which will cause inaccurate calculation. Assuming that the same section of the line is affected by external influences, the line shrinkage is uniform, and the ratio of the fault distance calculated actually to the length of the distribution line is equal to the ratio of the distance between the two towers to the total length of the line [29]. If the fault occurs at the time of t_0, the actual fault distance is calculated, as shown in (15):

$$\begin{cases} d'_{\mathrm{A}} = v\,(t_{\mathrm{A}} - t_0) \\ d'_{\mathrm{B}} = v\,(t_{\mathrm{B}} - t_0) \end{cases} \tag{15}$$

The actual length of the distribution line can be calculated as follows:

$$L' = d'_{\mathrm{A}} + d'_{\mathrm{B}} = v\,(t_{\mathrm{A}} - t_0) + v\,(t_{\mathrm{B}} - t_0) \tag{16}$$

According to the hypothesis, the distance from the fault point F to the end A is described as follows:

$$\begin{aligned} d_{\mathrm{A}} &= \frac{d'_{\mathrm{A}}}{L'} * L = \frac{v\,(t_{\mathrm{A}} - t_0)}{v\,(t_{\mathrm{A}} - t_0) + v\,(t_{\mathrm{B}} - t_0)} * L \\ &= \frac{t_{\mathrm{A}} - t_0}{t_{\mathrm{A}} - t_0 + t_{\mathrm{B}} - t_0} * L \end{aligned} \tag{17}$$

where:

t_0 is the time as the fault occurs;
t_{A} and t_{B} are the required time for the initial traveling wave of the fault transmitted to A and B, respectively.

It can be seen from (17) that the calculation of the fault distance is only related to t_0, t_{A}, t_{B}, and the line length L, independent of the traveling wave speed.

The power flow direction and operation mode in the traditional distribution network will be changed with DG access, however, the information of the wave head at the time of fault occurrence will not be affected [3]. With the traveling wave transmission process, there will be wave head attenuation. This phenomenon leads to inaccurate records of the second and third wave heads. For the proposed method of fault location in this research, the second and third wave heads do not need to be considered, and only the arrival moment of the first wave head needs to be recorded. In addition, due to the lack of line information in distribution network with DG access, it is difficult to obtain the parameters of the line accurately, which leads to the difficulty in the calculation of the theoretical value for the traveling wave velocity. The proposed method of fault location in this study does not need to calculate the velocity of traveling wave and the arrival time of reflected wave, and the calculation results are more accurate.

B. FAULT LOCATION PROCESS

A fault traveling wave signal will be generated in the fault point as the fault occurs in active distribution network, which will propagate along the different lines. In the process of transmission, refraction and reflection will occur while the fault point is encountered, which will produce non-stationary and non-linear signal. The VMD decomposition can decompose the signal effectively.

The traveling waves of the different phases will influence each other during the process of propagation due to the coupling phenomenon between the three-phase lines. Therefore, the signal needs to be decoupled to obtain three independent mode components before the VMD decomposition. In this study, Karenbell transform is employed for phase-to-mode transformation. The process of transformation can be expressed as follows:

$$\begin{bmatrix} I_\alpha \\ I_\beta \\ I_0 \end{bmatrix} = \frac{1}{3} \begin{bmatrix} 1 & -1 & 0 \\ 1 & 0 & -1 \\ 1 & 1 & 1 \end{bmatrix} \begin{bmatrix} \dot{I}_a \\ \dot{I}_b \\ \dot{I}_c \end{bmatrix} \tag{18}$$

where:

$\dot{I}_a$, $\dot{I}_b$, and $\dot{I}_c$ are the current information of each phase of the line, respectively;
I_α, I_β, and I_0 are α-mode, β-mode, and 0-mode, respectively, obtained after Karenbell transform.

The α-mode of the current signal is decomposed by IVMD after the decoupling transformation is completed. According to the number of decomposition layers, the mode components with the larger kurtosis value are selected for S-transform, and the high-frequency components in S- matrix are extracted to determine the time when the head of the fault traveling wave reaches each end point. Moreover, the fault distance is calculated by (17). The specific process is as follows:

1) Collect the information 5ms of three-phase current before and after the occurrence of the fault;
2) Karenbell decoupling the current information of 10,000 sampling points before and after the time of 5ms to obtain three modulus components;
3) Select the k value by using the method of the instantaneous frequency judgment, and VMD decomposition is performed;
4) Adopt the kurtosis criterion to select a suitable IMF for S-transform;
5) Extract the high frequency components in S-matrix, and determine the initial time when the fault traveling wave arrives at each end;
6) Perform the distance calculation by using (17).

The flow chart of the fault location is shown in Fig.3.

V. SIMULATION ANALYSIS

A. SIMULATION MODEL

In order to verify the effectiveness of the proposed algorithm, this research a multi-branch model for active distribution network with DG access is built, and simulation analysis is performed, shown in Fig.4. In the model, M_1 to M_7 are the end of each line, of which M_1 and M_4 are the end of the trunk line; the lines M_4T_4, T_2M_6 are the hybrid lines of overhead cable and the rest of the lines are overhead lines. Meanwhile, the parameters are the same in the same line.

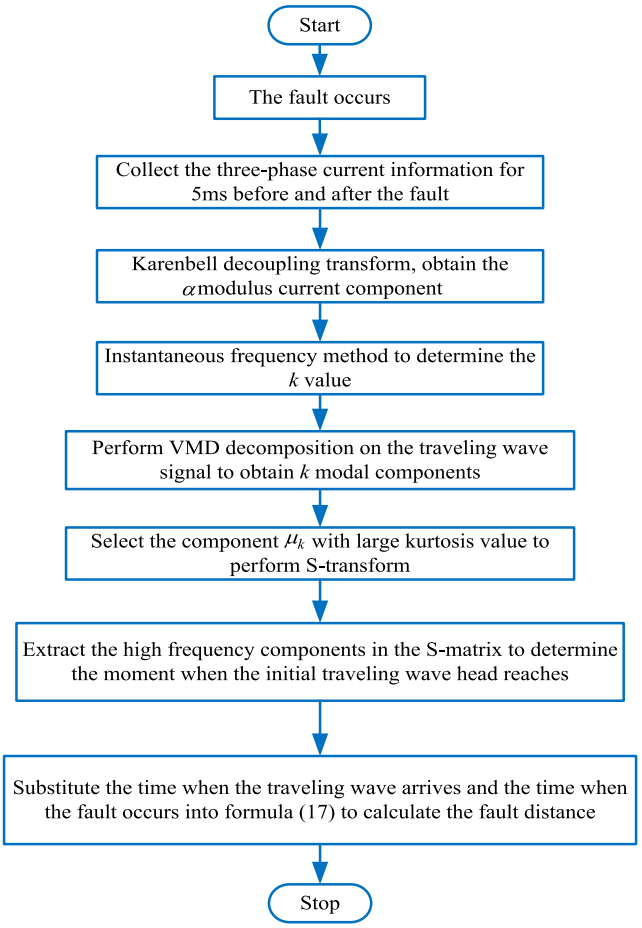

FIGURE 3. The flow chart of the proposed algorithm.

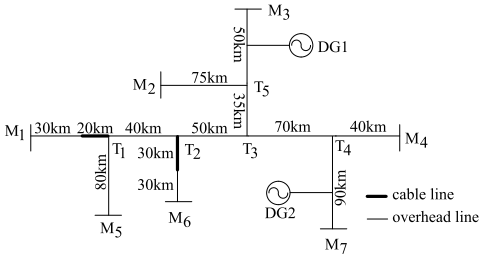

FIGURE 4. Multi-branch distribution line model with DG access.

One double fed induction generator (DFIG) of the capacity 3MW is connected to the branch M_3T_5, and four DFIGs of 1.5MW are connected to the branch T_4M_7.

The calculation formula for the penetration rate in the active distribution network can be expressed as follows [30]:

$$P_{\text{perm}} = \frac{P_{\text{DG-non}}}{P_{\text{Lsum}}} \tag{19}$$

where:

$P_{\text{DG-non}}$ is the total installed capacity of DG in the line;

P_{Lsum} is the total power of the loads in the line.

The total installed capacity of DG is 9MW, and the total load power is 13MW in the model. According to (19), the permeability of active distribution network is 69.23% which exceeds 60% about the concept of high penetration.

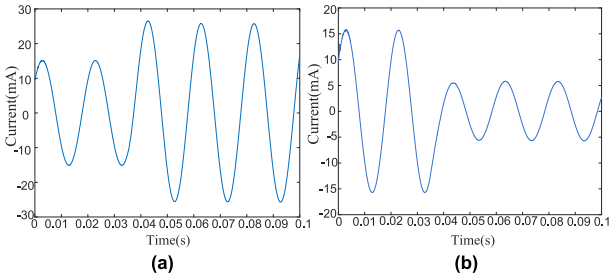

FIGURE 5. The α-mode current at the branch M_7T_4. (a) α-mode current at T_4. (b) α-mode current at M_7.

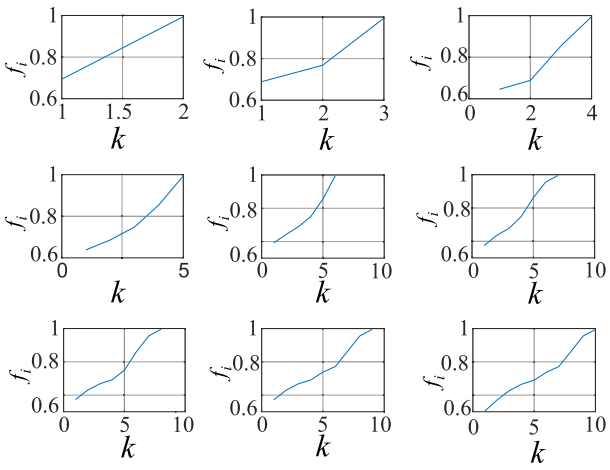

FIGURE 6. The mean value of the instantaneous frequency of each component in VMD.

B. SIMULATION RESULTS

The simulations of the different fault locations are carried out based on the model of active distribution system in Fig.4. It includes the analysis of three situations: M_iT_j branch fault, the fault between T nodes, and the fault on T nodes. The type of the fault is set to single-phase-to-ground. Moreover, the sampling frequency is 10kHz, the sampling time is 0.1s, and the time of the fault is 0.035s.

1) THE M_iT_J BRANCH FAULT

Assuming that the fault occurs in the branch M_7T_4, and the fault point is 35km away from the end T_4. The period 5ms of three-phase currents is collected before and after the fault, and Karenbell decoupling on the transient currents of 10,000 sampling points is performed to obtain the α-mode current, as shown in Fig.5.

The method of instantaneous frequency judgment is performed on the transient line mode current of the branch M_7T_4 obtained by decoupling to select the appropriate the value k. The value k is from 1 to 9 and nine curve graphs of instantaneous frequency average value can be obtained, as shown in Fig.6.

It shows in Fig.6, that the frequency f_i equals 1 if the value k equals 6. Meanwhile, the frequency k is always equal to 1 if the value k equals and more than 7, which shows that the

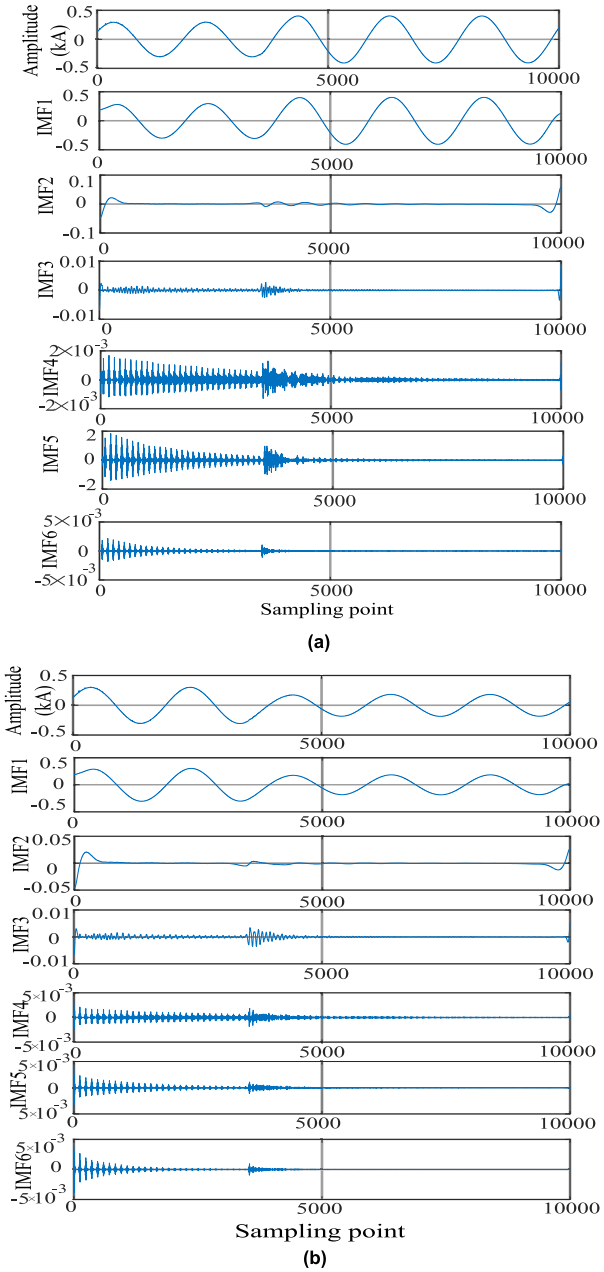

FIGURE 7. VMD decomposition of the fault branch M_7T_4. (a) VMD decomposition of the fault signal at the end T_4. (b) VMD decomposition of the fault signal at the end M_7.

TABLE 1. The kurtosis value of each component.

Endpoint	Ku1	Ku2	Ku3	Ku4	Ku5	Ku6
T_4	1.78	12.42	6.96	9.31	35.64	136.00
M_7	2.08	10.90	6.97	7.24	48.95	197.12

decomposition has reached the critical state. So the number 6 is selected as the value of k for VMD decomposition level. The decomposition is shown in Fig.7 (a) and Fig.7 (b).

The kurtosis values of six modal components at the end T_4 and the end M_7 are calculated by kurtosis criterion. The calculation results are shown in Table 1.

It can be seen from Table 1 that the kurtosis values of the sixth component at the end T_4 and the end M_7 are both

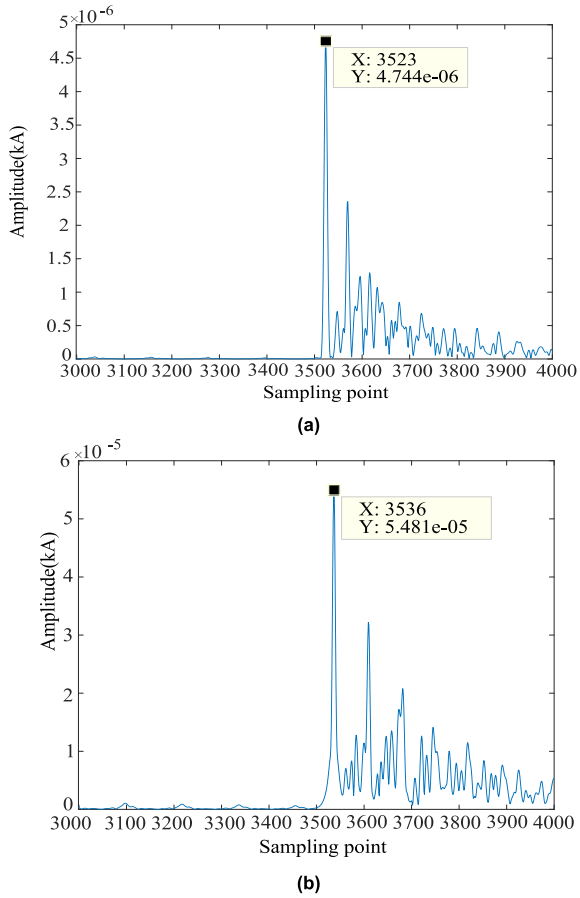

FIGURE 8. The diagram of time-frequency for S-transform at the branch M_7T_4. (a) The diagram of time-frequency for fault traveling wave at the end T_4. (b) The diagram of time-frequency for fault traveling wave at the end M_7.

the largest. Therefore, these components are selected for S-transform and the high-frequency components in S-matrix are extracted. As for the end T_4 and the end M_7, it is found that the maximum amplitude moment is between the sampling point of 3000 and 4000. The time-frequency information at 3000-4000 are extracted to obtain the arrival time of the initial fault traveling wave at the ends T_4 and M_7. The diagram of the time frequency for the fault traveling wave is shown in Fig. 8 (a) and Fig. 8 (b).

It is known in Fig.8(a) that the fault initial traveling wave arrives at the terminal T_4 at the 3523rd sampling point, and Fig.8(b) shows that the fault initial traveling wave arrives at the end M_7 at the 3536rd sampling point. Therefore, the timet_{T4} equals 0.03523s and t_{M7} equals 0.03536s. The time t_{T4} and t_{M7} are substituted into Eq.(18), and the fault distance$d$is calculated. The distance d is 35.085km and the absolute error is 85m.

The capacity of DG is changed while the total capacity of DG is 3MW. At the same time, the penetration rate of the active distribution network in this study is 23.08%. Moreover, the penetration rate is 46.15% while DG is connected to 6MW. The fault distances 15km, 30.5km, 35km and 65km away from the end T_4 are calculated respectively by changing

TABLE 2. The results of distance measurement if the fault happens at the branch M_7T_4.

Permeability (%)	Fault Distance(km)	Actual distance(km)	Absolute Error(m)
23.08	15	15.012	12
	30.5	30.508	8
	35	35.011	11
	65	64.990	10
46.15	15	15.019	19
	30.5	30.485	15
	35	35.014	14
	65	65.021	21
69.23	15	15.036	36
	30.5	30.569	69
	35	35.085	85
	65	64.920	80

the location of fault point in the branch line M_7T_4 so as to verify that the proposed algorithm can accurately locate the fault under the different permeability and fault distance. The results of fault location are shown in Table 2.

It can be seen from Table 2 that the proposed method can accurately measure the distance under the different fault locations and the different penetration rates while the single-phase-to-ground fault occurs on the line M_7T_4, and the absolute error is not more than 100m.

Assuming that the single-phase-to-ground fault occurs at the end M_1 near the end of the main line and the fault point is 50km away from the end M_1. Meanwhile, the penetration rate is 69.23%. According to the steps of the fault location at the branch M_7T_4, the time-frequency information from the sampling points of 3000 to 4000 in S-matrix is extracted to obtain the arrival time of the wave head for the initial traveling wave to at both ends of M_1 and T_1, as shown in Fig. 9.

According to Fig.9 (a) and Fig.9 (b), it can be concluded that the arrival time for the initial traveling wave to both ends of the fault are 0.03533s and 0.03520s, and the fault distance d equals 49.81km with the absolute error of 190m.

The fault distance under the different permeability is calculated while the distance between fault point and the end M_1 are 12.5km, 36.5km, 50km and 70km, respectively. The results are shown in Table 3.

As can be seen from Table 3, as the fault occurs in the branch M_1T_1, the fault distance can be calculated accurately with the absolute error within 200m under the different penetration rates and the different location from the fault point to the end.

2) THE FAULT BETWEEN T NODES

The fault of single-phase-to-ground happens between the nodes T_1 and T_2 as an example in order to analyze the fault between T nodes, and the fault distance between the fault point and the point T_1 are calculated as 10.5km, 25.5km and 55km, respectively, under the different permeability, as shown in Table 4.

According to Table 4, the proposed method in this study can accurately calculate the fault distance and the absolute error is within 150m as the location of the fault and the permeability are different.

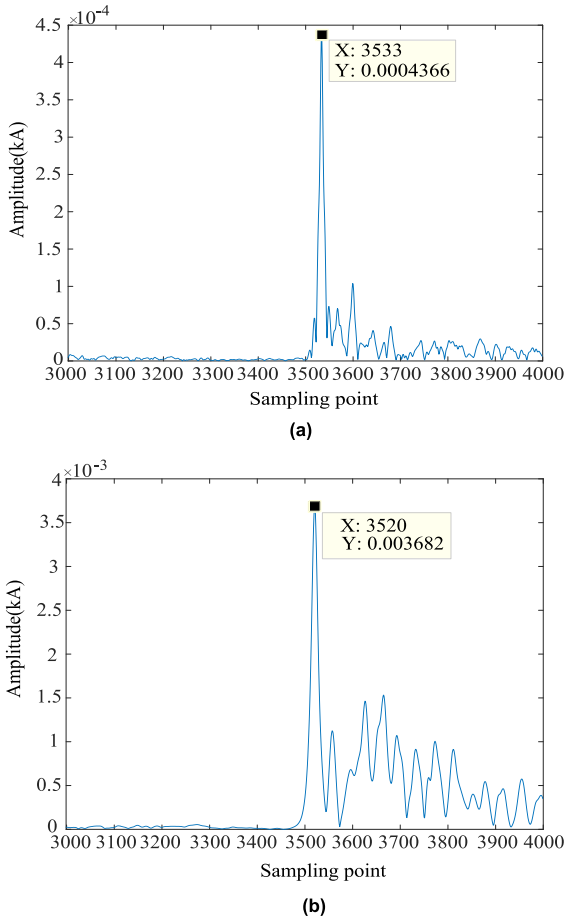

FIGURE 9. The diagram of time-frequency for S-transform at the branch M_1T_1. (a) The diagram of time-frequency for fault traveling wave at the end M_1. (b) The diagram of time-frequency for fault traveling wave at the end T_1.

TABLE 3. The results of distance measurement if the fault happens at the branch M_1T_1.

Permeability (%)	Fault Distance(km)	Actual Distance(km)	Absolute Error(m)
23.08	12.5	12.516	16
	36.5	36.489	11
	50	50.035	35
	70	70.064	64
46.15	12.5	12.531	31
	36.5	36.526	26
	50	50.100	100
	70	70.114	114
69.23	12.5	12.535	35
	36.5	36.541	41
	50	49.81	190
	70	70.135	135

3) THE FAULT ON T NODES

Assuming that the fault occurs at the node T_2 to analyze the condition of the fault occurrence on the node, and the fault distance is calculated under the different penetration rates from the two reference terminals T_1 and T_3. The results are expressed in Table 5.

According to Table 5, it shows that the fault distance is calculated from the ends T_1 and T_3 respectively if the fault occurs at the T_2 node, and the proposed method can calculate the distance accurately with the absolute error within 100m.

TABLE 4. The results of distance measurement if the fault happens at the T_1T_2.

Permeability (%)	Fault Distance(km)	Actual Distance(km)	Absolute Error(m)
23.08	10.5	10.521	21
	25.5	25.516	16
	55	54.978	22
46.15	10.5	10.462	38
	25.5	25.573	73
	55	55.100	100
69.23	10.5	10.541	41
	25.5	25.469	31
	55	54.890	110

TABLE 5. The results of distance measurement if the fault happens at the node T_2.

Permeability (%)	Reference terminal	Fault Distance(km)	Actual Distance(km)	Absolute Error(m)
23.08	T_1	70	70.015	15
	T_3	60	60.008	8
46.15	T_1	70	69.983	17
	T_3	60	60.012	12
69.23	T_1	70	70.081	81
	T_3	60	60.048	48

VI. CONCLUSION

In this study, a novel method of fault location in active distribution network based on the improved algorithm of VMD and S-transform is proposed, and it is applied to the multi-branch distribution lines with DG access. The following conclusions can be obtained:

(1) The fault traveling wave can be decomposed effectively by using the improved VMD decomposition, the kurtosis value of the modal components is calculated by the kurtosis criterion, and S-transform is performed on the optimal modal components. The proposed method improves the resolution of S-transform in time and the arrival time of the initial fault traveling wave to both ends of the fault line can be obtained more accurately;

(2) A model of the multi-branch distribution lines with DG access is built. The proposed algorithm can calculate the fault distance accurately for the faults at the branch, the fault between T nodes and the fault on T nodes under the different penetration rates, and the absolute error is within 200m;

(3) The proposed method in this study is independent of wave speed. Therefore, it is better to solve the problem that the calculation accuracy of the fault distance is easily affected by the velocity of traveling wave. At the same time, the S-matrix proposed in this paper makes the calculation accuracy higher. Because only the time of the initial wave head arriving at the detection point is selected, it is not affected by the fault distance and the reflected wave. Thus, the fault location is more reliable.

REFERENCES

[1] H. Wang, Y. Liu, B. Zhou, C. Li, G. Cao, N. Voropai, and E. Barakhtenko, "Taxonomy research of artificial intelligence for deterministic solar power forecasting," *Energy Convers. Manage.*, vol. 214, no. 15, pp. 112909.1–112909.17, Jun. 2020.

[2] L. Xi, L. Yu, Y. Xu, S. Wang, and X. Chen, "A novel multi-agent DDQN-AD method-based distributed strategy for automatic generation control of integrated energy systems," *IEEE Trans. Sustain. Energy*, vol. 11, no. 4, pp. 2417–2426, Oct. 2020.

[3] W. C. Santos, F. V. Lopes, N. S. D. Brito, and B. A. Souza, "High-impedance fault identification on distribution networks," *IEEE Trans. Power Deliv.*, vol. 32, no. 1, pp. 23–32, Feb. 2017.

[4] H. Wen, H. Yang, H. Kuang, X. Qin, and G. Cai, "Global threshold prediction of multicarrier multipactor with time distribution and material coefficients," *IEEE Trans. Electromagn. Compat.*, vol. 60, no. 5, pp. 1163–1170, Oct. 2018.

[5] D. Xu, Q. Wu, B. Zhou, C. Li, L. Bai, and S. Huang, "Distributed multi-energy operation of coupled electricity, heating, and natural gas networks," *IEEE Trans. Sustain. Energy*, vol. 11, no. 4, pp. 2457–2469, Oct. 2020.

[6] A. Hadaeghi, H. Samet, and T. Ghanbari, "Multi extreme learning machine approach for fault location in multi-terminal high-voltage direct current systems," *Comput. Electr. Eng.*, vol. 78, pp. 313–327, Sep. 2019.

[7] R. Benato, S. D. Sessa, M. Poli, C. Quaciari, and G. Rinzo, "An online travelling wave fault location method for unearthed-operated high-voltage overhead line grids," *IEEE Trans. Power Del.*, vol. 33, no. 6, pp. 2776–2785, Dec. 2018.

[8] Z. H. Dai and X. Wang, "Fault location algorithm of active distribution network based on improved impedance method," *Power Syst. Technol.*, vol. 41, no. 5, pp. 2027–2034, 2017.

[9] Y. S. Wang, S. Liu, and J. B. Yi, "Fault location algorithm based on state estimation in tree distribution network with distributed generation," *Power Syst. Protection Control*, vol. 46, no. 23, pp. 60–67, 2018.

[10] R. Dashti, M. Ghasemi, and M. Daisy, "Fault location in power distribution network with presence of distributed generation resources using impedance based method and applying π line model," *Energy*, vol. 159, no. 15, pp. 344–360, Sep. 2018.

[11] R. Chen, X. G. Yin, and Y. L. Li, "Fault location method for transmission grids based on time difference of arrival of wide area travelling wave," *J. Eng.*, vol. 2019, no. 16, pp. 3202–3208, Mar. 2019, doi: 10.1049/joe.2018.8459.

[12] X. Q. Liu, D. Z. Wang, and X. C. Wang, "Fault location algorithm for distribution power network based on relationship in time difference of arrival of traveling wave," *Proc. CSEE*, vol. 37, no. 17, pp. 4109–4115 and 4290, 2017.

[13] F. Deng, X. R. Li, and X. J. Zeng, "A novel multi-terminal fault location method based on traveling wave time difference for radial distribution systems with distributed generators," *Proc. CSEE*, vol. 38, no. 15, pp. 4399–4409 and 4640, 2018.

[14] X. Chen, X. G. Yin, X. Yin, J. R. Tang, and M. H. Wen, "A novel traveling wave based fault location scheme for power distribution grids with distributed generations," in *Proc. IEEE Power Energy Soc. Gen. Meeting (PESGM)*, Denver, CO, USA, 2015, pp. 1–5, doi: 10.1109/PESGM.2015.7286027.

[15] J. Ding, L. Li, Y. Zheng, C. Zhao, H. Chen, and X. Wang, "Distributed travelling-wave-based fault location without time synchronisation and wave velocity error," *IET Gener., Transmiss. Distrib.*, vol. 11, no. 8, pp. 2085–2093, Jun. 2017.

[16] S. Silva, P. Costa, M. Gouvea, A. Lacerda, F. Alves, and D. Leite, "High impedance fault detection in power distribution systems using wavelet transform and evolving neural network," *Electr. Power Syst. Res.*, vol. 154, pp. 474–483, Jan. 2018.

[17] X. Zhang, N. Tai, Y. Wang, and J. Liu, "EMTR-based fault location for DC line in VSC-MTDC system using high-frequency currents," *IET Gener., Transmiss. Distrib.*, vol. 11, no. 10, pp. 2499–2507, Jul. 2017.

[18] H. Boche and V. Pohl, "Calculating the Hilbert transform on spaces with energy concentration: Convergence and divergence regions," *IEEE Trans. Inf. Theory*, vol. 65, no. 1, pp. 586–603, Jan. 2019.

[19] K. Feng and X. L. Su, "Spatiotemporal characteristics of drought in the Heihe river basin based on the extreme-point symmetric mode decomposition method," *Int. J. Disaster Risk Sci.*, vol. 10, nos. 1–2, pp. 591–603, 2019.

[20] K. Dragomiretskiy and D. Zosso, "Variational mode decomposition," *IEEE Trans. Signal Process.*, vol. 62, no. 3, pp. 531–544, Feb. 2014.

[21] Y. Xu, Y. Gao, Z. Li, and M. Lu, "Detection and classification of power quality disturbances in distribution network based on VMD and DFA," *CSEE J. Power Energy Syst.*, vol. 6, no. 1, pp. 122–130, Mar. 2019.

[22] O. P. Mahela and A. G. Shaik, "Recognition of power quality disturbances using S-transform and rule-based decision tree," in *Proc. IEEE 1st Int. Conf. Power Electron., Intell. Control Energy Syst. (ICPEICES)*, New Delhi, India, Jul. 2016, pp. 1–6, doi: 10.1109/ICPEICES.2016.7853093.
[23] B. Zhu, F. Ding, and D. M. Vilathgamuwa, "Coat circuits for DC–DC converters to improve voltage conversion ratio," *IEEE Trans. Power Electron.*, vol. 35, no. 4, pp. 3679–3687, Apr. 2020.
[24] X. Zheng, Y. Wei, J. Liu, and H. Jiang, "Multi-synchrosqueezing S-transform for fault diagnosis in rolling bearings," *Meas. Sci. Technol.*, vol. 32, no. 2, Feb. 2021, Art. no. 025013.
[25] S. Lu, W. Wang, and G. Wang, "Stationary points of a kurtosis maximization criterion for noisy blind source extraction," *IEEE Access*, vol. 5, pp. 8736–8740, 2017.
[26] L. Xi, J. Wu, Y. Xu, and H. Sun, "Automatic generation control based on multiple neural networks with actor-critic strategy," *IEEE Trans. Neural Netw. Learn. Syst.*, early access, Jul. 14, 2020, doi: 10.1109/TNNLS.2020.3006080.
[27] Z. Tao, P. Zhaoming, and W. Min, "Early fault diagnosis method of rolling bearings based on VMD," *J. Beijing Univ. Tech.*, vol. 45, no. 2, pp. 103–110, 2019.
[28] R. G. Stockwell and L. Mansinha, "Localization of the complex spectrum: The S transform," *IEEE Trans. Signal Process.*, vol. 44, no. 4, pp. 998–1001, Apr. 1996.
[29] Y. F. Gao and Y. L. Zhu, "Study on lighting fault locating of high-voltage transmission lines based on VMD and TEO," *Trans. China Electrotech. Soc.*, vol. 31, no. 1, pp. 24–33, 2016.
[30] Y. C. Xu, S. R. Fan, C. Tan, and M. Lu, "Power quality disturbance detection and classification in high permeability active distribution network with improved EWT-CMPE," *Power Syst. Technol.*, vol. 44, no. 10, pp. 3991–4005, 2020.

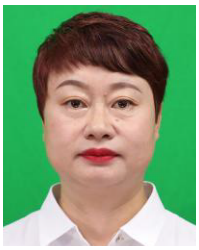

YANCHUN XU received the Ph.D. degree from the Department of Electrical Engineering, Harbin Institute of Technology (HIT), Harbin, China, in 2010.

She has worked at the China Three Gorges University, Yichang, China. Her research interests include disturbance signal detection with distributed generation, harmonics detection of power systems, as well as fault location with distributed generation access to distribution networks.

CAICAI ZHAO received the bachelor's degree from Wuchang Shouyi University, Wuhan, China, in 2018. She is currently pursuing the M.S. degree with the College of Electrical Engineering and New Energy, China Three Gorges University, Yichang, China.

Her research interests include fault location with active distribution networks.

SHASHA XIE received the bachelor's and M.S. degrees from the College of Electrical Engineering and New Energy, China Three Gorges University, Yichang, China.

Her research interests include voltage stability analysis, and distribution network operation and control.

MI LU (Senior Member, IEEE) received the M.S. and Ph.D. degrees in electrical and computer engineering from Rice University, in 1984 and 1987, respectively.

She is currently a Professor with Texas A&M University. Her research interests include digital system design and microprogrammed control of digital systems. She is a Senior Member of the IEEE Computer Society.